Available online at www.sciencedirect.com

ScienceDirect

Energy Procedia 49 (2014) 2462 – 2471

Energy Procedia

SolarPACES 2013

Performance analysis of offshore solar power plants

C. Diendorfer[a,]*, M. Haider[a], M. Lauermann[a]

[a]*Vienna University of Technology, Institute for Energy Systems and Thermodynamics, Getreidemarkt 9/302, 1060 Vienna, Austria*

Abstract

Large flat land surfaces, where direct normal irradiance (DNI) is high enough for concentrating solar power (CSP), are scarce in Europe. Floating offshore solar power plants in the Mediterranean Sea could increase the European solar power resources significantly. In this paper a solar collector platform design is investigated, where individual platform segments are supported by several air chambers, which are formed by cylindrical flexible membrane skirts. This paper is focused on the optical performance of the collector platform which is simulated in a dynamic model. Two types of concentrators are considered: (1) Parabolic Trough Collectors and (2) Pneumatic Pre-Stressed Solar Concentrators. From experimental data gained from a 4x4 m physical model, we have obtained the general characteristics of the platform. Using wave data of the Mediterranean Sea, the motion of the platform in different sea states is calculated. The dependency of the concentrator system on the angle of incident, which is in this case also a function of the platform motion due to ocean waves, is obtained from ray tracing. Solar irradiance is derived from satellite data and also included in the model. Combining all these data in one dynamic model, the achievable optical performance of a floating offshore solar power plant is calculated as a function of time and location.

Selection and peer review by the scientific conference committee of SolarPACES 2013 under responsibility of PSE AG.
Final manuscript published as received without editorial corrections.
Keywords: Offshore Solar Power, Floating Solar Power Plant, Performance Analysis

1. Introduction

Concentrating Solar Power (CSP) requires large flat areas with high direct normal irradiance (DNI). This type of landscape is scarce in Europe. If the ocean surface in the Mediterranean Sea could be used for solar power generation, Europe's solar power resources could be increased significantly. Building solar power plants offshore offers two technical advantages. First sun-tracking around a vertical axis can be implemented easily. This simplifies

* Corresponding author. Tel.: +43-1-58801-302331; fax: +43-1-58801-302399.
E-mail address: christian.diendorfer@tuwien.ac.at

Selection and peer review by the scientific conference committee of SolarPACES 2013 under responsibility of PSE AG.
Final manuscript published as received without editorial corrections.
doi:10.1016/j.egypro.2014.03.261

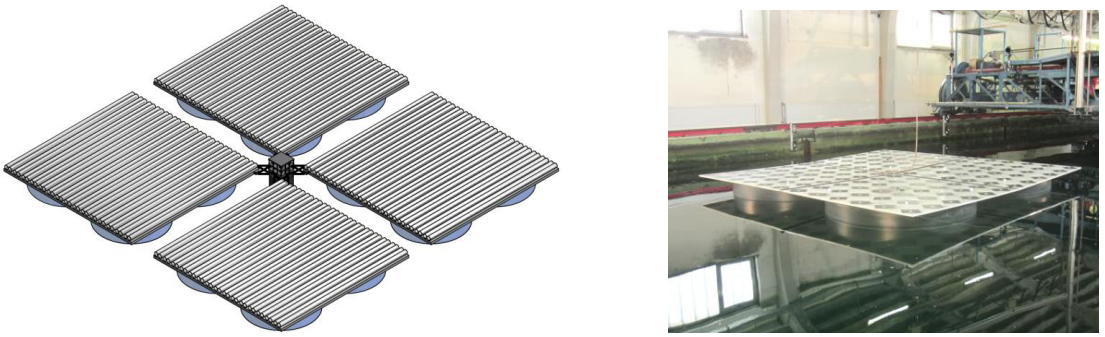

(a) (b)

Fig. 1. (a) Conceptual design with four solar fields (b) Physical model of one solar field

the requirements for the concentrator systems and avoids shading between collector rows. By revolving the entire platform around a vertical axis, a tracking system for each collector row is not required. Secondly unlimited cooling water is available, which can increase the efficiency of the thermodynamic cycle. These two advantages could lead to a cost reduction compared to land based systems and counterbalance the extra costs for going offshore. As a challenge the platform has to withstand wave and wind forces, which lead to platform motion. Especially when CSP is used on a floating platform, the motion has to be as small as possible in order to maintain focus of the concentrators. Even small deflections of the platform would lead to a misalignment of the mirrors to the sun [1].

To keep electricity production costs competitive, the platform design itself has to be cost efficient. For the conceptual design, which is investigated in this paper, this is achieved by building the collector fields as a lightweight structure on several air chambers, which are formed by cylindrical flexible membrane skirts. The air cushions provide the required buoyancy and decrease the wave excitation of the platform. Weights are fixed to the bottom end of the skirts to stabilize the membranes and guarantee for air tightness. The collector fields are connected to a power island, on which the steam turbine, condenser, auxiliary equipment and optional heat storage are located. Fig. 1 (a) shows a design drawing of the platform concept.

In this paper a model is presented, which calculates the optical efficiency of this platform design for a given location and time.

2. Model setup

The goal of the presented model is the combination of different data sets and mathematical models to calculate the achievable power output. The platform motion at different sea states is described by experimental data, the environmental conditions at the Mediterranean Sea is gained from satellite data and a wave atlas. The optical behavior of the concentrator systems under the influence of platform motion is investigated by ray tracing.

2.1. Environmental conditions

The weather conditions at the installation site of a solar power plant are crucial for the power output. For the performance of an offshore solar power plant two parameters are very important: Solar irradiation and the sea state. Until now CSP plants were only designed for onshore usage. Therefore detailed direct solar irradiance (DNI) data is only available for onshore locations. Feasible DNI data for the Mediterranean Sea in this project are derived from the surface solar irradiance dataset from [2]. This dataset is based on the International Satellite Cloud Climatology Project (ISCCP) and contains daily mean values of global horizontal irradiance (GHI) for the entire world in a 0.5

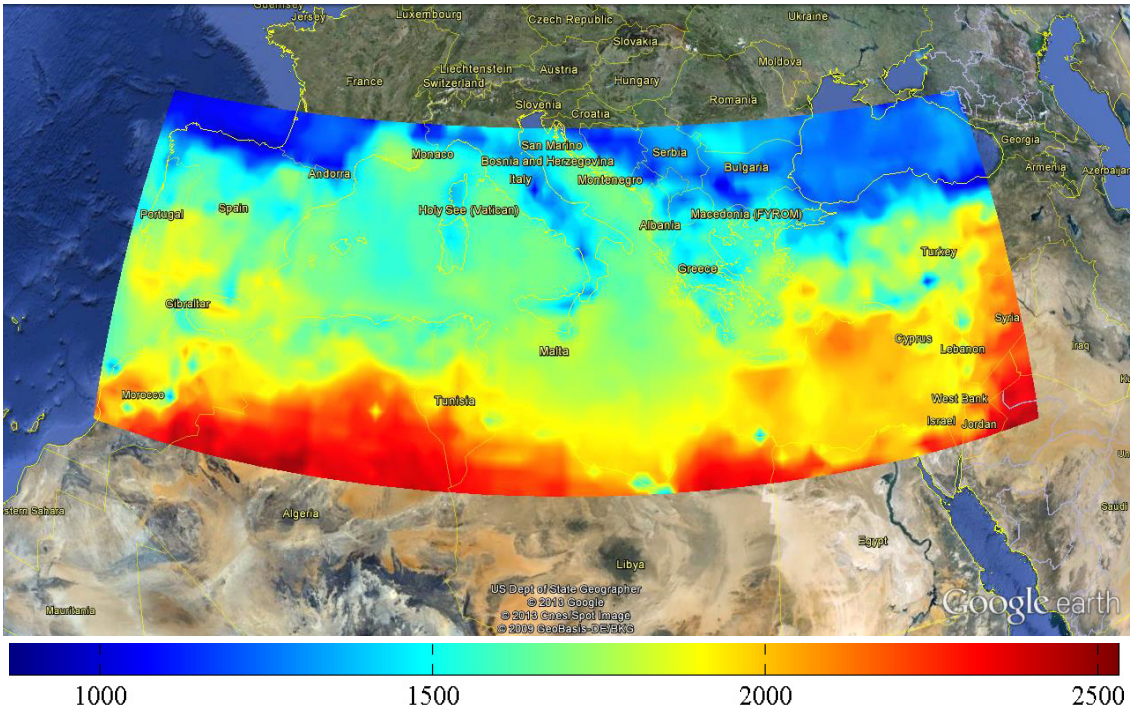

Fig. 2. Direct normal irradiance in kWh/m^{2}a for the Mediterranean region

degree resolution for the time period from 1991 until 1993. More details about this data set and the method of deriving GHI from the satellite data can be found in [3, 4, 5]. To get a better temporal resolution, hourly GHI values are derived from the daily GHI values. This is done by using the model presented in [6]. The model calculates the relationship between hourly and daily GHI as a function of day length, which is a function of location and time. The model is not an exact process, but it will work best for clear days, and those are the days that will produce most power output.

GHI is the sum of direct and diffuse irradiance. Only direct irradiance can be concentrated. Therefore DNI has to be calculated from the GHI values. This is done by using the Direct Insolation Simulation Code (DISC) [7]. The DISC model calculates the ideal clear sky irradiance for a given location at a given time and compares it with the measured values. From this comparison DISC can estimate the atmospheric conditions at the measurement site and calculates the DNI values using empirical formulas.

By combining these data and methods a data set is created, which contains hourly DNI values for the Mediterranean region in a 0.5 degree resolution for a three year time period (1991 – 1993). Fig. 2 shows the mean annual direct normal irradiation for the region of interest, derived from the created data set. One can see in Fig. 2 that the annual direct normal irradiation at offshore regions is higher than at most European land regions. The annual direct normal irradiation of this data set was compared with data from HelioClim-3 [8], which can be found at [9]. The results match well for the region of interest.

The time variable sea state is another important factor for the performance of an offshore solar power plant. Using wave data, which can be found in [10], the most probable sea states in the Mediterranean Sea can be derived. In Fig. 3 one can see the data which was derived from the wave atlas. Fig. 3 (a) is a wave scatter diagram and shows the frequency occurrence of sea states, which are defined by the significant wave height H_s and mean wave period T_m. In Fig. 3 (b) the frequency of occurrence of different wave directions is presented. 80% of the sea states have a H_s smaller than 2 m and a T_m smaller than 6 s. The main wave direction is between 90° and 135°. In this paper results for a sea state with H_s = 2 m and T_m = 6 s, which should model typical operating conditions, and for a sea state with H_s = 4 m and T_m = 8 s are presented. H_s = 4 m and T_m = 8 s equate to storm conditions and only 3% of the

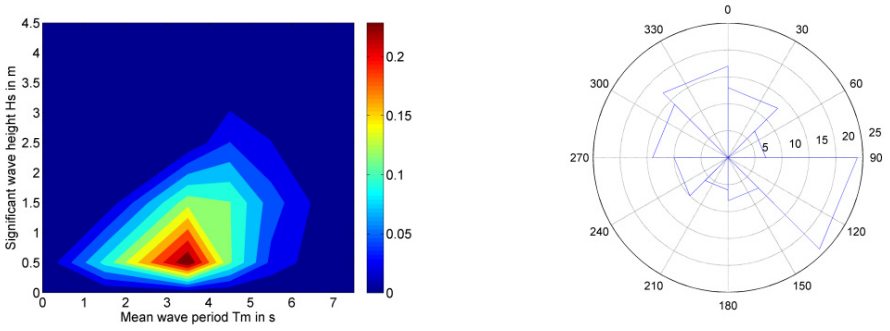

(a) (b)

Fig. 3. (a) Wave scatter diagram for Mediterranean Sea (b) Frequency of occurrence of wave directions in percent

sea states are worse than the one mentioned. DNI will be very low under storm conditions and therefore the efficiency of the platform under these conditions will not have an impact to the overall performance. Nevertheless this sea state is calculated with the developed model to investigate the platform's behavior under severe conditions.

2.2. Platform motion

The main dimensions of the platform have been designed by a mathematical model, which is based on methods described in [11] and calculates the average and the maximum response of a platform design to typical Mediterranean Sea states. Several designs of different dimensions were created and investigated by this model. It was learned that the skirt diameter is the most important design parameter. A physical model of the most promising design, shown in Fig. 1 (b), was built and tested at Vienna Model Basin. Three sets of measurements for 0°, 22.5° and 45° wave heading were performed. Each set contains 10 regular wave frequency measurements. From the regular wave measurements the response amplitude operators (RAOs) [12] of the platform were gained. The RAOs are basically the frequency responses of the platform and characterize the platform motion in ocean waves. The RAOs are complex numbers, which describe the ratio between ocean wave amplitude and the platform response amplitude and the phase shift between the wave and the response signal.

RAOs for the six degrees of freedom and three deformation modes of the platform were gained from the measurements. Only the rotational degrees of freedom are considered in the model, as the translational degrees of freedom have no influence on the power plant performance. Fig. 4 shows the definition of the three rotational degrees of freedom and the deformation modes. X-direction is defined parallel to the absorber tube axis.

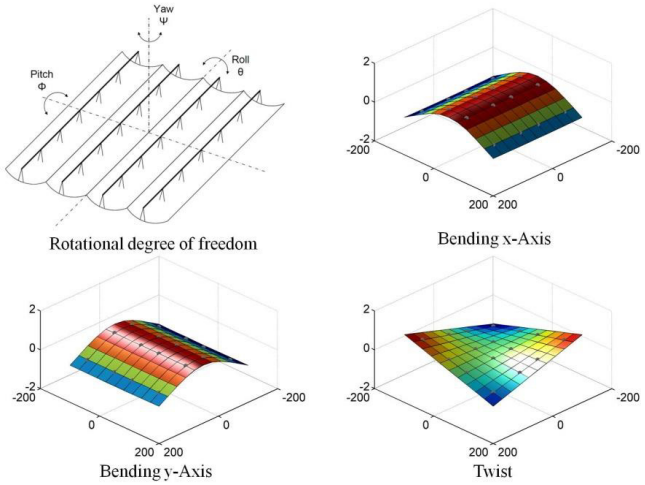

Fig. 4. Rotational degrees of freedom and deformation modes

To calculate the platform motion under ocean wave influence, a random wave signal is generated. First a JONSWAP energy density spectrum **S**(f) [13] as a function of wave frequency f for desired H_s and T_m is calculated. Fig. 5 (a) shows an example of the rotational RAOs and a wave spectrum **S**(f) with a mean wave period of 6 s. One can see in Fig.5 that the RAOs are small at the frequency where the wave spectrum has its energy peak. This will result in a very low platform response. The energy density spectrum is converted to a wave height spectrum **H**(f) by equation (1) [12] where Δf is the bandwidth of the discretization.

$$\mathbf{H}(f) = 2 \cdot \sqrt{2 \cdot S(f) \cdot \Delta f} \tag{1}$$

As the phase angles between the motion in the rotational degrees of freedom and deformation modes are important, random phase angles θ are generated for each Fourier component of the time signal. By adding the phase angles to **H**(f) a random wave signal is defined, which has the desired spectral parameters. The phase angles are added according to equation (2).

$$\underline{\mathbf{H}}(f) = \mathbf{H}(f) \cdot e^{i\Theta} \tag{2}$$

The complex height spectrum $\underline{\mathbf{H}}$(f) of the wave signal is multiplied with the RAOs to obtain the complex response height spectra $\underline{\mathbf{H}}_{\mathbf{R}}$(f). For each degree of freedom and deformation mode a response height spectrum is calculated. From the complex response height spectra the platform motion in the time domain can be derived by equation (3).

$$\eta(t) = \sum_n \left| \frac{\underline{H}_R(f_n)}{2} \right| \cdot \cos(2\pi f_n t + \Theta_{Rn}) \tag{3}$$

In equation (3) η(t) is the platform deflection for the considered degree of freedom or deformation mode at the time t, f_n is the frequency, and θ_{Rn} is the response phase angle of the Fourier component n. Fig. 5 (b) presents an example of the model process. It is a cutout of a pitch motion signal of the platform and the corresponding water elevation. The motion of the degrees of freedoms and deformation modes are superposed to get the total platform motion.

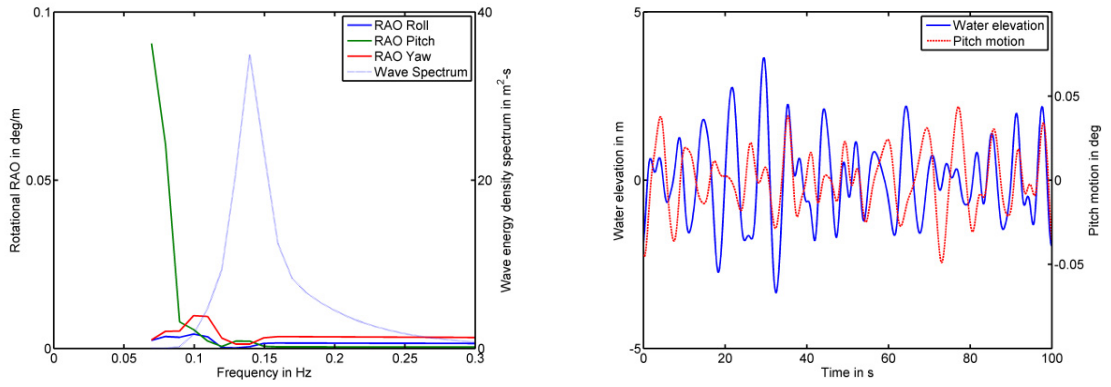

(a) (b)

Fig. 5. (a) Rotational RAOs and wave spectrum (T_m = 6s) (b) Water elevation and pitch motion

2.3. Concentrator system

The efficiency of solar concentrators depends highly on the correct alignment of the concentrators to the sun. Usually the misalignment is small and results from manufacturing and installation imprecision. On an offshore power plant additional misalignment results from platform motion. Currently two types of concentrators are considered to be installed on an offshore platform: Conventional Parabolic Trough Concentrators (PTC) and Pneumatic Pre-stressed Concentrators (PPC). Pneumatic Pre-stressed Concentrators are air filled tubes with two chambers, which are divided by a mirror foil. By setting the correct pressure ratio between the two chambers, the mirror foil gets a circular shape and concentrates the incoming sun light to the absorber tube. PPCs are a light weight construction, which is a major advantage for offshore platforms. On the other hand side the efficiency of PPCs is slightly smaller than for PTC, which results from the circular mirror shape instead of a parabolic. As reference design for PTC system the EuroTrough collector [14] is selected. The geometry for the PPC system is based on the design presented in [15] and scaled to an aperture width of 5.77 m, for better comparability with the PTC system.

For both systems the optical efficiency η_{opt} is calculated. The optical efficiency includes reflection losses of the mirror, transmission losses of the absorber glass envelope, the absorbance of the receiver, end losses and geometry errors. All used values can be found in [16]. For PPC additionally transmission losses from the upper transparent foil are included. As some of these losses depend on the angle of incident, the platform motion is already partially included in the optical efficiency. The main influence of platform motion is included in the cosine loss and the intercept factor. For a horizontal land based system with vertical tracking, the cosine loss only depends on the solar elevation angle. For a floating offshore platform the cosine loss results from the superposition of the solar elevation angle and the platform's pitch angle. The intercept factor γ is defined as

$$\gamma = \frac{n_{receiver}}{n_{total}} \tag{4}$$

where $n_{receiver}$ is the number of rays hitting the absorber and n_{total} is the number of rays reflected by the mirror. Fig. 6 shows the dependency of the intercept factor on the transversal angle of incident for several PTC and PPC geometries. The design, which is displayed with the bold red line, is used in the presented model. The ray tracing model which was used to calculate the intercept factors is described in [1].

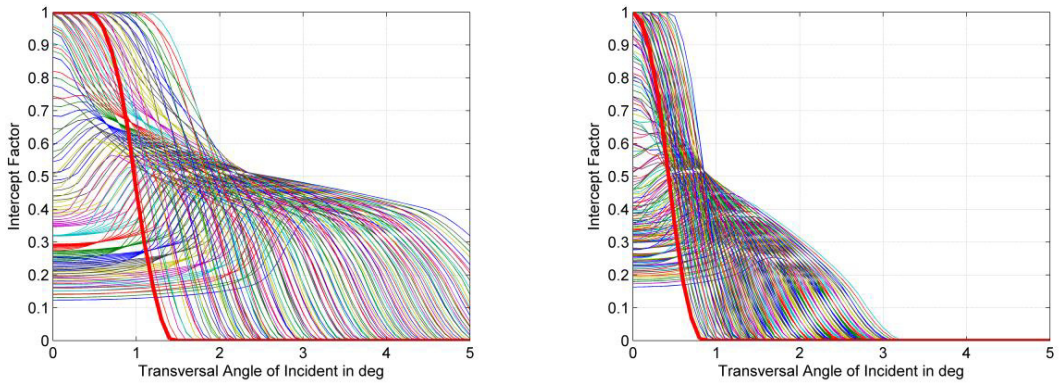

(a) (b)

Fig. 6. Dependency of the Intercept factor for (a) PTC and (b) PPC designs to the transversal angle of incident. [1]

2.4. Efficiency calculation

To calculate the platform's efficiency for a specific date and location, the sun's path for this time period and location is calculated using formulas found in [6]. By combining the platform motion with the concentrator model and the sun position, the efficiency of the platform can be calculated. The platform is discretized into 10x10 elements. For each time step the normal vector of each element is calculated and transformed from a local coordinate system to a global South-East-Upwards coordinate system. The transformation from the local coordinate system to the global coordinate system is done by the usage of Euler angles. Euler angles work well in the current case, as the deflection from the neutral position is small. In Fig. 7 the discretized platform and the normal vectors for one time step are shown. Red areas are deflected upwards and blue areas are deflected downwards from the neutral position.

From the sun's elevation angle α_s and azimuth angle γ_s, a vector pointing towards the sun can be calculated for each time step using equation (5).

$$\mathbf{n_s} = \begin{pmatrix} \cos\alpha_s \cos\gamma_s \\ -\cos\alpha_s \sin\gamma_s \\ \sin\alpha_s \end{pmatrix} \tag{5}$$

The angle between the element's normal vector and the sun vector $\mathbf{n}_s$ equals the angle of incident Θ_s in the concentrator model. The angle of incident is calculated for each platform element. For the calculation of the intercept factor the transversal angle of incident has to be used. It is calculated in a local coordinate system, in which the absorber axis defines the x-direction and the normal vector of the platform element defines the z-direction. The y-direction is derived from the cross product of the x and y axis. The solar radiation per square meter aperture area q_{abs}, which is absorbed from the absorber tube, is calculated according to equation (6).

$$q_{abs} = DNI \cdot \cos\Theta_s \cdot IAM \cdot \eta_{opt} \cdot \gamma \tag{6}$$

In equation (6) DNI is the direct normal irradiance in W/m^2 and IAM is the Incident Angle Modifier. As all discrete elements of the platform have the same size, the average radiation for the entire platform is calculated for each time step. Then the average irradiation at the absorber per hour is calculated, which is the output of the model.

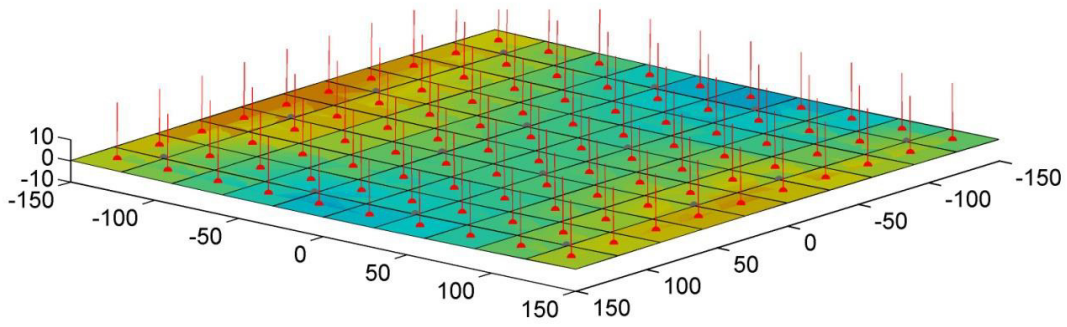

Fig. 7. Discretized platform and normal vectors. Red areas are deflected upwards, blue areas are deflected downwards from neutral position

3. Results

The results presented in this paper are calculated for June, 21st at a location in the Mediterranean Sea south of Malaga, Spain for wave spectra with the parameters H_s = 2 m, T_m = 6 s (typical operating conditions) and H_s = 4 m, T_m = 8 s (storm conditions). All time values presented are in local time and not in solar time. The wave heading is varied from 0° (North) to 90° (East) in 22.5° steps. Due to the symmetry of the square platform, this covers all possible wave directions.

The wave direction has an influence on the platform efficiency, as the platform rotates around a vertical axis over the day in order to follow the sun. For wave directions of 0° and 180° the main motion of the platform at solar noon would be a pitch motion. When the platform is pitched towards the sun, the cosine and end losses are decreased. When the platform is pitched in the other direction, cosine and end losses are increased. As the average position of the platform is horizontal, a pitch motion has no influence on the performance. For wave directions of 90° and 270° the platform would fulfill a roll motion at solar noon. The roll motion has an influence on the transversal angle of incident and therefore on the intercept factor. Misalignments in transversal direction sum up independently of their direction.

Fig. 8 shows the efficiency of the two investigated concentrator designs for operating and storm conditions. The efficiency is defined as the ratio between the actual amount of energy absorbed by the collector tubes and the solar energy arriving at the mirrors. By multiplying the efficiency with the DNI values, the energy which is transferred to the heat transfer fluid in the absorber tubes can be calculated. For comparison with the floating platform an ideal platform is calculated, which does not fulfill any motions due to wave excitation. It only rotates around a vertical axis to track the sun. This platform is called “land based” system in Fig. 8.

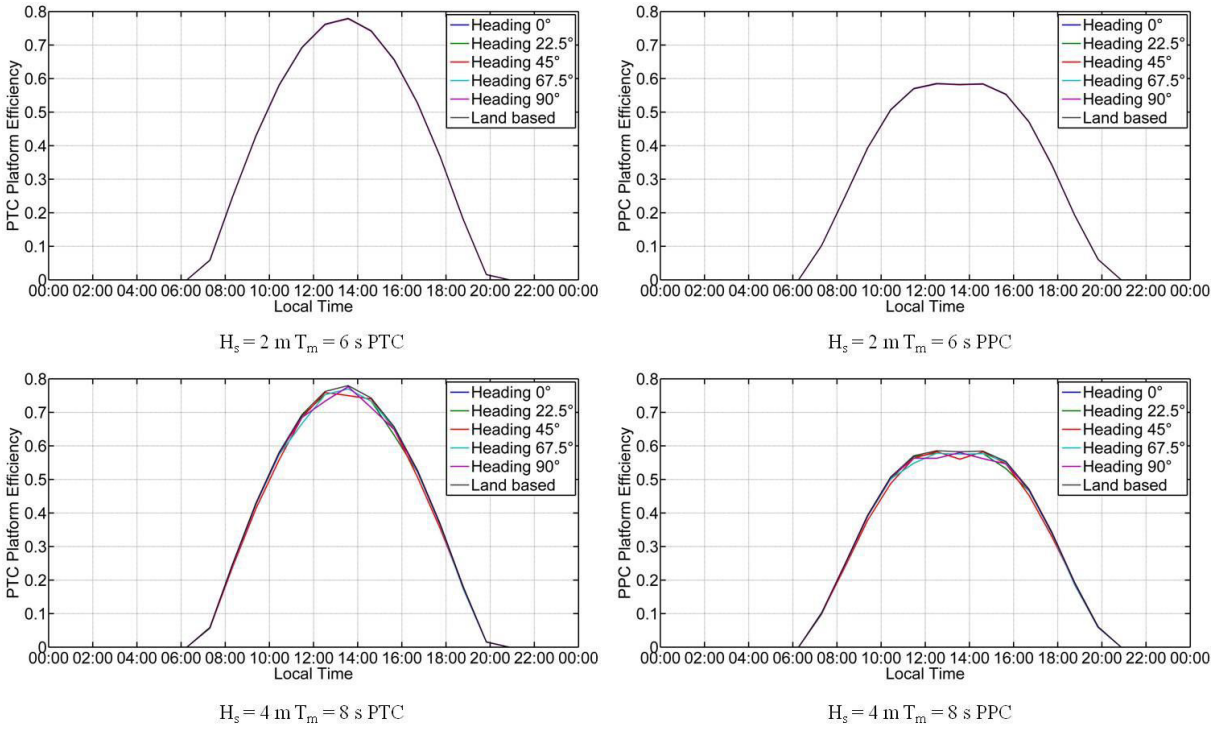

Fig. 8. Efficiencies of a PTC and a PPC platform located south of Malaga, Spain on June, 21st for different wave directions

The platform is designed in a way, that responses to typical waves during operating conditions are as small as possible. Therefore platform motions due to wave excitation have almost no influence on the overall performance of the system. Under storm conditions the performance of the floating systems is slightly lower than that of the land based system. Under operating conditions the influence of the wave heading is almost not visible. The influence of the wave direction can be seen for stormy conditions, but as DNI is usually low during stormy weather the influence of the wave direction can be neglected in further investigations.

4. Conclusion

In this paper the influence of sea wave excitation on the performance of floating offshore solar power plants is investigated. The avoidance of platform motion is essential for an economic platform design, as the efficiency of solar concentrators decreases significantly for even small misalignments [1]. Therefore a platform design was developed, which reduces the platform response to wave excitation to a minimum. It is demonstrated that wave motion and direction have theoretically an influence on the performance, but as the effect is very small for the presented design, we conclude that it can be neglected in further investigations. The performance is a function of the time depending sea state. In typical operating conditions platform motion due to wave excitation has an insignificant influence on the performance, which gives proof of an appropriate platform design. In rougher sea states the influence increases, but as DNI usually decreases in stormy weather conditions, the performance loss compared to land based systems will be small. From the analysis presented in this paper it can be concluded that from a technical point of view floating offshore solar power plants may be a feasible contribution to Europe's power supply. The floating stability of the presented platform design has been validated both numerically and experimentally and the performance impact for going offshore is small.

As the conceptual design of the platform is now validated, further investigations seem appropriate. In the next steps detailed questions concerning the designs of the power island and of the platforms will be analyzed. Capex, operation and maintenance are key factors. For the concentration system PPC is prioritized, as it promises automatic alignment, low cost and better protection against saline environment. Concerning Capex, first detailed calculations based on the finite element method yielded that there is a justified hope that the area weight of PPC concentrator platforms can be kept below 50kg/m2.

Acknowledgements

The financial support by the Austrian Research Promotion Agency (FFG) within the program "Research Studio Austria" is gratefully acknowledged.

References

[1] Diendorfer C, Haider M, Lauermann M. Nummerical simulation of the optical performance of offshore solar power plants. SolarPaces Proceedings 2012

[2] Lamont-Doherty Earth Observatory, Columbia University. (2000). Bishop's High-resolution (DX) surface solar irradiance derived. Research Data Archive at the National Center for Atmospheric Research, Computational and Information Systems Laboratory. http://rda.ucar.edu/datasets/ds741.1. Accessed 20/03/2013.

[3] Bishop J, Rossow W, Dutton E. Surface solar irradiance from the Internationa Satellite Cloude Climatology Project 1993-1991. Journal of Geophysical Research, Vol. 102, 1997

[4] Bishop J, Russow W. Spatial and temporal veriability of global surface solar irradiance. Journal of Geophysical Research, Vol. 96, 1991

[5] Frouin R, Lingner D, Gautier C. A simple analytical formula to compute clear sky total and photoynthetically available solar irradiance at the ocean surface. Journal of Geophysical Research, Vol. 94, 1989.

[6] Duffie J, Beckman W. Solar Engineering of Thermal Processes, John Wiley & Sons, 2006.

[7] Maxwell E. A quasi-physical model for converting hourly global horizontal to direct normal insolation. SERI Report No. SERI/TR-215-3087, Solar Energy Research Institute,1987

[8] Rigollier C, Lefèvre M, Wald L. The method Heliosat-2 for deriving shortwave solar radiation data from satellite images. Solar Energy, 77(2), 159-169, 2004.
[9] IRENA. Global Solar and Wind Atlas. irena.masdar.ac.ae. Accessed 21/05/2013.
[10] Caires S, Sterl A, Komen G, Swail V. Global wave climatology atlas derived form 45-years of ECMWF reanalysis data. www.knmi.nl/waveatlas. Accessed 20/03/2013.
[11] Chakrabarti S. Handbook of Offshore Engineering Volume 1. Elsevier, 2005.
[12] Chakrabarti S. Offshore Structure Modeling. Advanced Series on Ocean Engineering – Volume 9, World Scientific, 1994.
[13] DIN Deutsches Institut fuer Normung e.V. Petroleum and natural gas industries – Specific requirements for offshore structures – Part1: Metocean design and operation considerations. EN ISO 19901-1:2005, 2006.
[14] Geyer C et al. EuroTrough – Parabolic Trough Collector Developed for Cost Efficient Solar Power Generation, 11th Int. Symposium on Concentrating Solar Power and Chemical Energy Technologies, Zurich, Switzerland, 2002.
[15] Hartl M, Ponweiser K, Haider M, Höfler J. Modeling of a Pneumatic Pre-Stressed Solar Concentrator based on Polymeric Membranes, ASME-ATI-UIT Thermal and Environmental Issues in Energy Systems 2010, 721-725, 2010.
[16] Forristall R. Heat Transfer Analysis and Modeling of a Parabolic Trough Solar Receiver Implemented in Engineering Equation Solver, Technical Report NREL/TP-550-34169, 2003.